4962–4969 *Nucleic Acids Research, 1997, Vol. 25, No. 24*

Interaction of minor groove binding ligands with long AT tracts

Anita Abu-Daya[+] and Keith R. Fox*

Division of Biochemistry and Molecular Biology, School of Biological Sciences, University of Southampton, Bassett Crescent East, Southampton SO16 7PX, UK

Received August 26, 1997; Revised and Accepted October 20, 1997

ABSTRACT

We have used quantitative DNase I footprinting to examine the ability of distamycin and Hoechst 33258 to discriminate between different arrangements of AT residues, using synthetic DNA fragments containing multiple blocks of $(A/T)_6$ or $(A/T)_{10}$ in identical sequence environments. Previous studies have shown that these ligands bind less well to $(A/T)_4$ sites containing TpA steps. We find that in $(A/T)_6$ tracts distamycin shows little discrimination between the various sites, binding ~2-fold stronger to TAATTA than $(TA)_3$, T_3A_3 and GAATTC. In contrast, Hoechst 33258 binds ~20-fold more tightly to GAATTC and TAATTA than T_3A_3 and $(TA)_3$. Hydroxyl radical footprinting reveals that both ligands bind in similar locations at the centre of each AT tract. At $(A/T)_{10}$ sites distamycin binds with similar affinity to T_5A_5, $(TA)_5$ and AATT, though bands in the centre of $(TA)_5$ are protected at ~50-fold lower concentration than those towards the edges. Hoechst 33258 shows a similar pattern of preference, with strong binding to AATT, T_5A_5 and the centre of $(TA)_5$. Hydroxyl radical footprinting reveals that at low concentrations both ligands bind at the centre of $(TA)_5$ and A_5T_5, while at higher concentrations ligand molecules bind to each end of the $(A/T)_{10}$ tracts. At T_5A_5 two ligand molecules bind at either end of the site, even at the lowest ligand concentration, consistent with the suggestion that these compounds avoid the TpA step. Similar DNase I footprinting experiments with a DNA fragment containing T_n (n = 3–6) tracts reveals that both ligands bind in the order $T_3 < T_4 << T_5 = T_6$.

INTRODUCTION

Distamycin and Hoechst 33258 are members of a group of compounds that bind to the minor groove of AT-rich regions of double-stranded DNA. They have been widely studied as model compounds for sequence-specific recognition of DNA (1,2). These ligands fit snugly within the DNA minor groove, where they interact with between three and five AT base pairs. GC base pairs are excluded from the binding sites as a result of steric clash with the guanine 2-amino group.

Distamycin and netropsin are oligopeptide antibiotics containing three or two pyrrole rings respectively. Their preference for AT base pairs has been well established by several footprinting studies (3–7). Netropsin requires a target site of four AT base pairs, while distamycin binds optimally to five contiguous AT base pairs, on account of its larger size. The crystal structure of netropsin bound to CGCGAATTCGCG (8,9) shows the crescent-shaped compound bound to the central AATT, with its three amides facing the floor of the groove, forming two sets of bifurcated hydrogen bonds with N3 of adenine and O2 of thymine. Van der Waals interactions with the wall of the narrow minor groove stabilize the complex and contribute to the specificity of the ligand. The structure of netropsin bound to CGCGATATCGCG is different is several respects (10), in particular, instead of the bifurcated hydrogen bonds the molecule is anchored by single hydrogen bonds between the amide NH groups and the O2 of adenine and the N3 of thymine.

Footprinting studies have shown that distamycin is more tolerant of a GC base pair at the end of the binding site (6,7,11). Both distamycin and netropsin bind to $d(A)_n \cdot d(T)_n$ more tightly than $d(AT)_n$ (12) and, in common with other minor groove binders, the presence of TpA (but not ApT) reduces the binding affinity (13). Distamycin binds to CGCAAATTTGCG in a unique configuration and covers the sequence AAATT (14).

In addition to these simple complexes, several recent studies have shown that in sequences containing five or more AT residues two distamycin molecules can bind simultaneously, forming a side-by-side 2:1 complex (15–18). The cooperative formation of 2:1 complexes depends on the sequence of the target site; no 2:1 complexes are observed with sequences which adopt a narrow minor groove, such as AAAAA (19), while only 2:1 complexes are formed at sequences with wider minor grooves and increased flexibility, such as ATATA (20). Although 2:1 complexes can be formed at AAATTT (21), the side-by-side model has not been observed in crystal structures with this sequence (10).

Footprinting studies with Hoechst 33258 indicate that the drug covers at least four AT base pairs, though a GC can be accommodated at the end of the binding site. TpA steps weaken the binding (22,23). Although Hoechst 33258 binds to the same sequences as netropsin and distamycin, its precise location need not be the same (22). Affinity cleavage studies of Hoechst analogues have also shown that small changes in sequence environment can alter its relative affinity for different binding sites (24,25). The selectivity of this ligand is emphasized in an NMR study with GGTAATTAC, in which it is bound in a unique position across the central AATT, even though several other AT binding modes are theoretically possible (26).

*To whom correspondence should be addressed. Tel: +44 1703 594374; Fax: +44 1703 594459; Email krf1@soton.ac.uk

[+]Present address: 430 Clinical Research Building, University of Pennsylvania, 415 Curie Boulevard, Philadelphia, PA 19104, USA

Table 1. Sequences of DNA inserts

Name	Sequence
$A_{3–6}$	CGCGTTTTTTCGCGTTTTTCGCGTTTTCGCGTTTCGCG
AT_6	CGCGAAATTTCGCGTATATACGCGTAATTACGCGTTTAAACGCGAATTCGCG
AT_{10}	CGCGTTTTTAAAAACGCGTATATATATACGCGAAAAATTTTTCGCGAATTCGCG

These inserts were cloned into the *Bam*HI site of pUC18. The strand shown is the one seen on labelling the DNA fragment at the 3′-end of the *Hin*dIII site.

Our previous footprinting studies have shown that for sites containing four consecutive AT base pairs, AAAA and AATT are stronger binding sites than TTAA and TATA (27). The differences in binding to various AT tracts were interpreted in terms of changes in the DNA minor groove width and suggest that TpA steps within an AT tract decrease ligand affinity. These differences were more pronounced for Hoechst 33258, which showed a 50-fold difference in binding to AATT and TATA compared with a 5-fold difference for distamycin. Since these studies investigated $(A/T)_4$ tracts they only concerned the 1:1 binding mode. In this paper we examine the interaction of distamycin and Hoechst 33258 with DNA fragments containing longer (A/T) tracts with the aim of understanding the ability of these ligands to discriminate between different arrangements of AT residues.

MATERIALS AND METHODS

Chemicals and enzymes

Distamycin and Hoechst 33258 were purchased from Sigma and stored at –20°C as 10 mM stock solutions in 10 mM Tris–HCl, pH 7.5, containing 10 mM NaCl. DNase I was purchased from Sigma and stored at –20°C as a stock solution of 7200 U/ml. These were diluted to working concentrations immediately before use. All other DNA modifying enzymes were purchased from Promega. Oligonucleotides were purchased from Oswel.

DNA plasmids

Plasmids containing synthetic DNA inserts were prepared as previously described. Synthetic oligonucleotides were treated with polynucleotide kinase, annealed and ligated into the *Bam*HI site of pUC18. The ligation mixture was transformed into *Escherichia coli* TG2. Successful clones were picked as white colonies from agar plates containing X-gal and IPTG. The sequences of the inserts were confirmed using a T7 sequencing kit (Pharmacia) and are shown in Table 1.

DNA fragments

Labelled DNA fragments containing the inserts were prepared by digesting the plasmids with *Hin*dIII, labelling at the 3′-end with [α-^{32}P]dATP using AMV reverse transcriptase and cutting again with *Eco*RI or *Sac*I. Since the inserts AT_6 and AT_{10} contain internal *Eco*RI sites (GAATTC) this could not be used as the second enzyme. Radiolabelled DNA fragments of interest were separated from the remainder of the plasmid on non-denaturing 8% (w/v) polyacrylamide gels. The isolated DNA fragments were dissolved in 10 mM Tris–HCl, pH 7.5, containing 0.1 mM EDTA so as to give 10–20 c.p.s./µl as determined on a hand held Geiger counter. For these experiments the absolute DNA concentration is not important, so long as it is smaller than the dissociation constant of the DNA binding ligand. We estimate that the strand concentration was <10 nM in all experiments.

DNase I footprinting

Radiolabelled DNA fragments (1.5 µl) were mixed with 1.5 µl ligand, dissolved in 10 mM Tris–HCl, pH 7.5. The complexes were allowed to equilibrate at room temperature (20°C) for at least 30 min before digestion with 2 µl DNase I (0.01 U/ml, dissolved in 1 mM $MgCl_2$, 1 mM $MnCl_2$, 20 mM NaCl). In each case the ligand concentration refers to that in the complex before addition of the enzyme. The digestion was stopped after 1 min by adding 3.5 µl DNase I stop solution (80% formamide containing 10 mM EDTA). Samples were heated at 100°C for 3 min before electrophoresis.

Hydroxyl radical footprinting

Radiolabelled DNA (3 µl) was mixed with 3 µl ligand, dissolved in 10 mM Tris–HCl, pH 7.5, containing 10 mM NaCl and left to equilibrate for 30 min at room temperature (20°C). Hydroxyl radical digestion was initiated by adding 6 µl freshly prepared solution containing 30 µM ferrous ammonium sulphate, 60 µM EDTA, 1 mM ascorbic acid and 0.1% hydrogen peroxide. The reaction was allowed to proceed for 10 min before stopping by adding 8 µl 1 M sodium acetate and 65 µl ethanol. The precipitate was washed with 70% ethanol, dried and redissolved in 6 µl 80% formamide containing 10 mM EDTA.

Gel electrophoresis

Products of DNase I and hydroxyl radical digestion were resolved on 10% (w/v) polyacrylamide gels containing 8 M urea and run at 1500 V for ~2 h. The gels were then fixed in 10% (v/v) acetic acid before drying at 80°C and subjected to autoradiography at –70°C using an intensifying screen. Bands were assigned by comparison with Maxam–Gilbert markers specific for G+A.

Data analysis

Autoradiographs of DNase I digestion patterns were scanned using a Hoefer GS365 microdensitometer. For the analysis we chose a band in each site which was well resolved and cut well in the control. The intensity of each band was estimated using the manufacturer's software. Footprinting plots (28) were constructed from these data and C_{50} values, indicating the ligand concentration which reduced the band intensity by 50%, were derived by fitting a simple binding curve to plots of band intensity against ligand concentration using FigP for Windows (Biosoft). These were fitted to equation **1**.

$$I_c = I_0(C_{50}/(L + C_{50}) \quad \mathbf{1}$$

where I_c is the band intensity in the presence of the ligand, I_0 is the band intensity in the control and L is the ligand concentration. The use of this equation to analyse footprinting data requires that the experiments are performed under conditions of single hit kinetics and assumes that the DNA concentration is very low (much lower than the dissociation constant of the ligand). Under these conditions for single binding sites C_{50} is equal to the thermodynamic dissociation constant. For longer AT sites the C_{50} value will represent the dissociation constant, averaged over the contiguous overlapping sites. Standard errors of the C_{50} values for each curve were calculated by the fitting routine and were obtained as the square roots of the variances found on the diagonal of the covariance matrix. In some instances the fit of the hyperbolic curve to the experimental data is not good and is presumed to result from a combination of errors in the quantitation, the overlap of potential binding sites and the presence of secondary binding modes. The accuracy of the data do not warrant the introduction of more complex binding equations which introduce further binding parameters. It should also be noted that comparison of sites *within* each DNA fragment is more reliable than comparison of sites *between* different fragments.

RESULTS

Previous footprinting studies (27) showed that for sites containing four consecutive AT residues distamycin binds to AATT more tightly than ATAT, TATA, TAAT and TTAA, with a 5-fold difference in affinity between the strongest and weakest sites. Hoechst 33258 displays greater selectivity, binding to AATT ~50 times more tightly than to TTAA and TATA. The results were interpreted by suggesting that these ligands bind to narrow minor grooves, avoiding the TpA step. We were therefore interested to determine whether these ligands could distinguish between different arrangements of AT residues in longer AT tracts.

Six consecutive AT residues

The first two panels of Figure 1 show DNase I digestion patterns of fragment AT_6 in the presence and absence of distamycin and Hoechst 33258. This fragment contains four different arrangements of $(A/T)_6$ residues together with AATT, for comparison with previous work. These AT tracts are separated by CGCG, thereby placing them in identical sequence environments. Since the different arrangements of $(A/T)_6$ residues are contained within a single DNA fragment it is relatively simple to compare the affinities of a ligand for the various sites. Looking first at the patterns with distamycin, it can be seen that the ligand produces a footprint at each of the AT sites at a concentration of <1 μM. Visual inspection of these patterns suggests that TAATTA represents the best binding site; bands in this region are attenuated at ~0.1 μM, in contrast to the other sites, which are not affected until 0.3–0.4 μM. An estimate of the relative affinities for the different sites was obtained by densitometric analysis of bands in these patterns, producing the C_{50} values presented in Table 2. These confirm that TAATTA is the best site, with a C_{50} value half that at the other sites, which have similar affinities. No data can be determined for A_3T_3 since DNase I cleavage in this region is too poor. It should also be noted that distamycin concentrations >3 μM cause a general inhibition of DNase I cleavage, with a few regions of enhanced cutting at the 3′-(lower) edge of $(TA)_3$ and below the AATT site in the sequence TCTC; these enhancements were excluded from the quantitative analysis.

Table 2. C_{50} values (μM) for distamycin and Hoechst 33258 binding to various AT sites

DNA fragment	Site	Distamycin	Hoechst
AT_6	$(TA)_3$	0.25 ± 0.12	1.04 ± 0.25
	TAATTA	0.107 ± 0.025	0.057 ± 0.010
	T_3A_3	0.28 ± 0.10	0.84 ± 0.24
	AATT	0.20 ± 0.06	0.057 ± 0.023
AT_{10}	AATT	0.084 ± 0.009	0.0037 ± 0.0006
	T_5A_5	0.158 ± 0.047	0.031 ± 0.007
	$(TA)_5$-1	nd	0.70 ± 0.15
	$(TA)_5$-2	0.063 ± 0.027	0.307 ± 0.054
	$(TA)_5$-3	0.058 ± 0.028	0.085 ± 0.015
	$(TA)_5$-4	0.059 ± 0.012	0.151 ± 0.031
	$(TA)_5$-5	0.071 ± 0.015	1.59 ± 0.32
	$(TA)_5$-6	4.06 ± 1.45	5.11 ± 1.30
$A_{3–6}$	T_6	0.085 ± 0.039	0.064 ± 0.007
	T_5	0.082 ± 0.031	0.053 ± 0.007
	T_4	0.125 ± 0.030	0.098 ± 0.040
	T_3	2.43 ± 0.49	1.23 ± 0.45

The parameters were derived from simple binding curves fitted to plots of band intensity against ligand concentration as described in Materials and Methods. The values are quoted ± SE describing the errors estimated from fitting the binding curve to at least eight data points. The data were obtained in 10 mM Tris–HCl, pH 7.5, containing 10 mM NaCl and were derived from densitometer scans of the autoradiographs presented in Figures 1, 3 and 6. For AT_{10} six bands within $(TA)_5$ were analyzed, as shown in Figure 3. These are numbered from the bottom to the top of the site and correspond to the sequence $CGCGTA^6TA^5TA^4TA^3TA^2CG^1CG$.
nd, not determined.

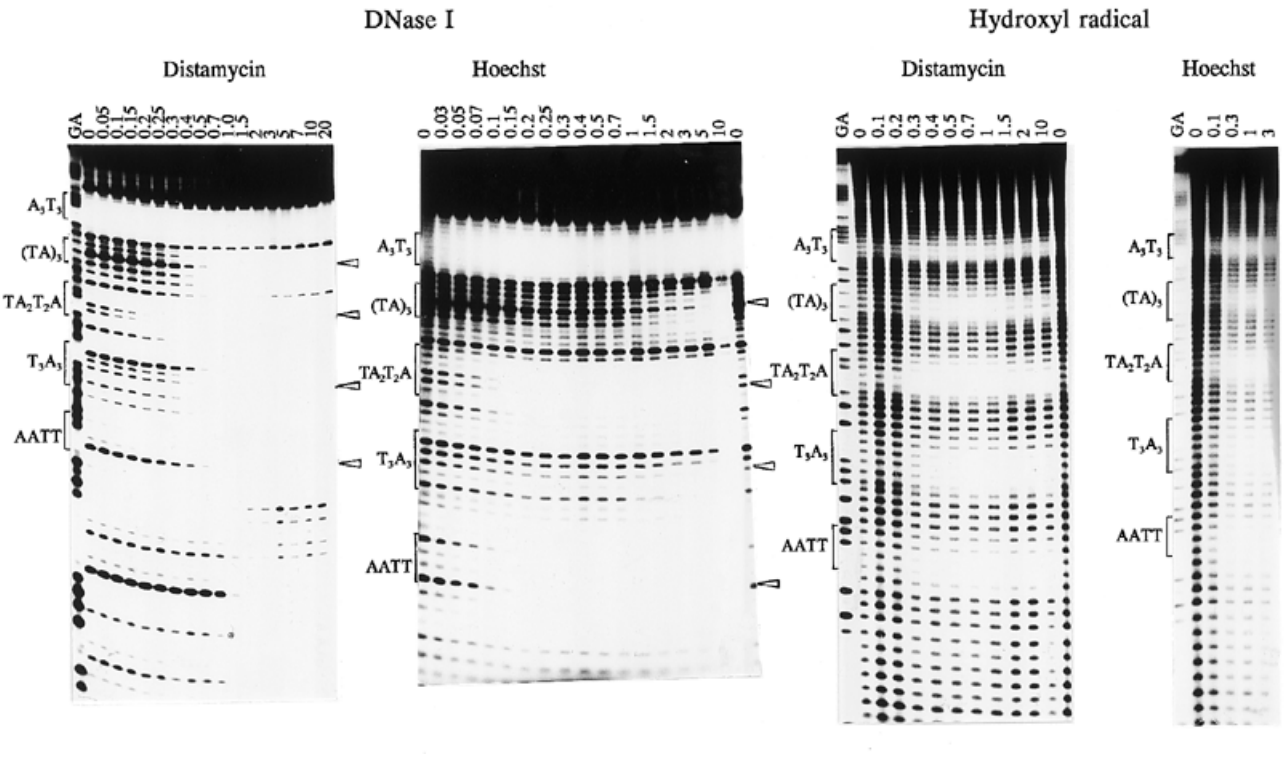

Figure 1. DNase I and hydroxyl radical cleavage patterns of fragment AT_6 in the presence of distamycin and Hoechst 33258. Ligand concentrations (μM), calculated before addition of the enzyme, are indicated at the top of each lane. The position of each of the AT tracts is shown by the square brackets. Tracks labelled GA are marker lanes specific for purines. In the DNase I digests the arrows indicate the bands that were considered for quantitative analysis.

The second panel of Figure 1 shows the results of a similar experiment with Hoechst 33258. It is immediately apparent that footprints at AATT and TAATTA are produced by 0.1 μM ligand, while T_3A_3 and $(TA)_3$ require much higher concentrations. This is confirmed by quantitative analysis of bands within these target sites generating C_{50} values, which are presented in Table 2. These show that Hoechst 33258 binds to TAATTA and AATT ~20-fold more tightly than to T_3A_3 and $(TA)_3$. Once again no data are available for A_3T_3.

Although DNase I is a useful footprinting agent for determining the relative affinities of these ligands for different binding sites it is a large molecule which produces uneven cleavage patterns. It is therefore not a good probe for determining the exact location and size of each binding site. In this regard a much better probe is the hydroxyl radical which, on account of its smaller size, produces a more even ladder of cleavage products. The results of hydroxyl radical cleavage experiments are presented in the third and fourth panels of Figure 1. Visual inspection of the patterns in the presence of distamycin reveals that three to four bands are protected from cleavage in each AT tract. This can be seen more clearly in the densitometer traces shown in Figure 2. As expected for an agent that cuts from the DNA minor groove, the protection is staggered towards the 3′-end of each site. The protection patterns at each site are very similar, suggesting that although the affinity of the ligand may depend on the precise arrangement of AT residues, the ligand is bound in the same location within each AT site. Quantitative footprinting data are harder to obtain from these hydroxyl radical digests, but visual inspection of the patterns is consistent with the results of DNase I cleavage; in particular, complete protection at T_3A_3 and $(TA)_3$ requires slightly higher distamycin concentrations than the other sites. In addition, clear protection can be seen at A_3T_3, a site for which no information was obtained with DNase I. Similar experiments with Hoechst 33258 reveal that attenuation of cleavage at AATT, TAATTA and A_3T_3 at low ligand concentrations is more pronounced than at $(TA)_3$ and T_3A_3. However, inspection of the densitometer traces shown in Figure 2 reveals a similar pattern to that produced by distamycin, in which the ligand occupies approximately the same position at each AT site. It therefore appears that differences in affinity for the various sites do not arise from variations in the binding mode or ligand position.

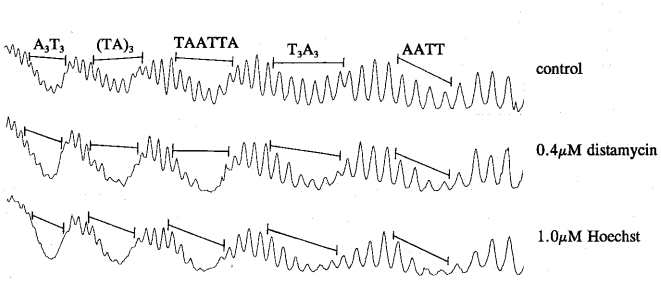

Figure 2. Densitometer scans showing hydroxyl radical cleavage of fragment AT_6 in the presence and absence of distamycin and Hoechst 33258. The position of each AT tract is indicated.

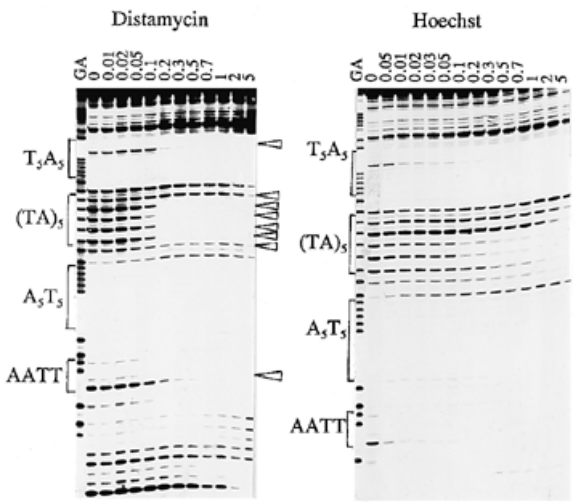

Figure 3. DNase I cleavage of fragment AT_{10} in the presence of distamycin and Hoechst 33258. Ligand concentrations (μM) are indicated at the top of each lane. The position of each of the AT tracts is shown by the square brackets. Tracks labelled GA are marker lanes specific for purines. In the first panel the arrows indicate the bands that were considered for quantitative analysis.

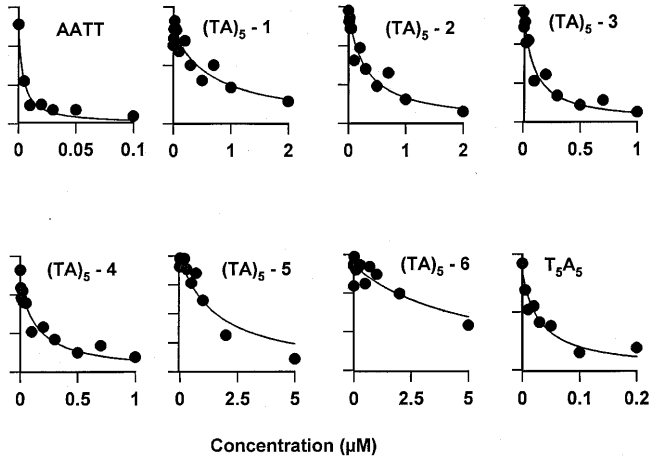

Figure 4. Footprinting plots showing the interaction of Hoechst 33258 with various sites within the fragment AT_{10}. The intensity of each band was determined from densitometer scans of the autoradiographs shown in Figure 3. The six bands used for $(AT)_5$ are numbered from the bottom to top of the gel. The ordinate shows the Hoechst concentration (μM); the abscissa shows the bands intensity (arbitrary units). The curves correspond to the binding parameters shown in Table 2.

Ten consecutive AT residues

We have extended these studies by examining the interaction of distamycin and Hoechst 33258 with fragment AT_{10}, which contains three different arrangements of 10 consecutive AT base pairs together with AATT, separated by four GC base pairs (CGCG) as in AT_6. Figure 3 (first panel) presents DNase I digestion patterns of this fragment in the presence of increasing concentrations of distamycin. It can be seen that in the AATT site the band corresponding to cleavage of TpC becomes fainter at 0.2 μM distamycin and gradually disappears until a clear footprint is evident at 0.7 μM. The A_5T_5 region is resistant to DNase I digestion, so that no information can be gained about interaction with this site. In the $(TA)_5$ site the four central marked bands, corresponding to the three lower ApT steps and the following ApC, show noticeable attenuation at 0.2 μM distamycin and a clear footprint at 0.3 μM. Cleavage of the flanking regions is only attenuated at concentrations >1 μM. It should be remembered that since DNase I acts in the minor groove, all these footprints are shifted by 2–3 bp to the 3′-(lower) side of the actual binding site. This may therefore suggest that at low concentrations distamycin binds in the centre of the $(TA)_5$ tract, but at higher concentrations the entire site is occupied, presumably by two (or more) ligands. In the T_5A_5 region one strong band is evident, corresponding to cleavage of the last TpT step. Cleavage at this step is almost completely blocked at 0.2 μM distamycin. Densitometric analysis of these cleavage sites yielded the C_{50} values shown in Table 2. It appears that these sites do not show the wide range of affinities seen with shorter $(A/T)_4$ sites (27) and that T_5A_5 is only marginally weaker than AATT. In addition, the previous studies showed that TATA is a much weaker site than AATT, whereas in these longer AT sites there is no difference in binding to the centre of $(TA)_5$ and AATT. It appears that when TATA is flanked by other TpA steps it is equivalent to AATT.

The second panel of Figure 3 shows the results of similar experiments with Hoechst 33258. It can be seen that cleavage of the TpC step in AATT is attenuated at very low ligand concentrations (0.005 μM). Digestion of A_5T_5 is again too weak to detect any interactions with the ligand. Protection of $(TA)_5$ requires higher ligand concentrations (≥0.1 μM). Bands towards the centre of this site are protected at lower concentrations than those at the edges, as observed with distamycin. The first and second (uppermost) ApT steps are only protected at the highest concentration (5 μM). At the highest concentration used the footprint with Hoechst is larger than that with distamycin. Cleavage within the T_5A_5 site is attenuated at the lowest ligand concentration. Quantitative analysis of these autoradiographs produced the footprinting plots shown in Figure 4 and the C_{50} values presented in Table 2 and confirm the rank order of affinities as AATT > T_5A_5 > $(TA)_5$. This is consistent with the previous data with $(A/T)_4$ sites, which showed that Hoechst binds very strongly to AATT and has the lowest affinity for TATA (27).

The interaction of distamycin with AT_{10} was also investigated using hydroxyl radicals and the results are presented in Figure 5a. Although hydroxyl radical cleavage of the drug-free control lanes is not even, showing attenuated cleavage in the AT tracts as a result of their narrower minor grooves, clear footprints can be seen in each of the AT tracts in the presence of distamycin. However, the protection pattern at A_5T_5, $(TA)_5$ and T_5A_5 changes in a concentration-dependent fashion. At higher antibiotic concentrations bands can be seen in the centre of these regions which are not present at lower concentrations. These changes are more clearly seen in the densitometer traces presented in Figure 5b. With 0.05 μM ligand $(TA)_5$, A_5T_5 and AATT show a single region of reduced cleavage which is biased towards the 3′-end of each AT tract. In the presence of 1 μM distamycin the cleavage pattern at each of these sites changes so that two or three new bands are evident towards the centre of the longer AT tracts

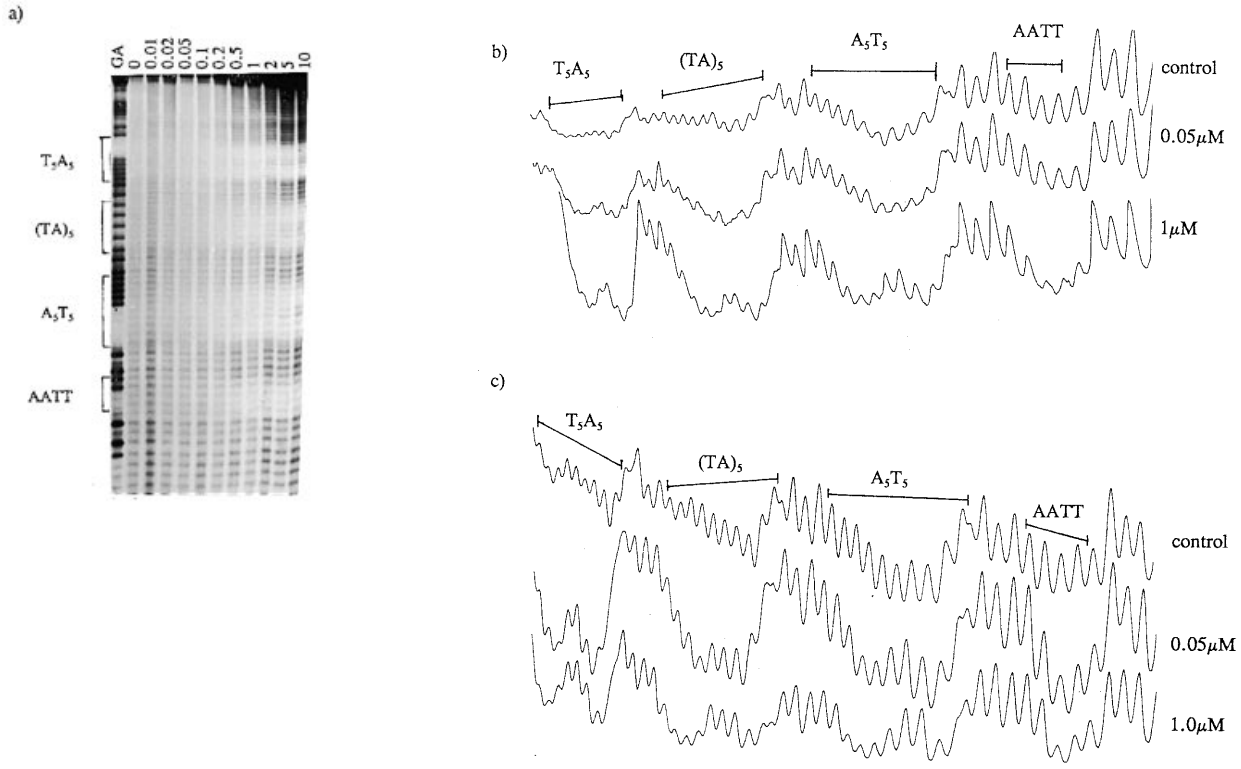

Figure 5. (**a**) Hydroxyl radical cleavage of fragment AT_{10} in the presence of various concentrations of distamycin. Ligand concentrations (μM) are shown at the top of each gel lane. The track labelled GA is a marker specific for purines. (**b**) Densitometer scans derived from the autoradiograph shown in (a) in the absence and presence of 0.05 and 1 μM distamycin. (**c**) Densitometer traces of hydroxyl radical cleavage of fragment AT_{10} in the absence and presence of 0.05 and 1.0 μM Hoechst 33258.

(but not AATT). It seems likely that this arises because more than one ligand is able to bind to each of these long AT tracts. At low ligand concentrations only one ligand molecule is bound, which appears to be preferentially located at the centre of each AT tract. At higher concentrations this will be replaced by two ligand molecules, binding closer to the edges of the AT tracts, leaving a central region which is less protected from hydroxyl radical cleavage. This effect is not seen at AATT as this site is only large enough to accommodate one ligand molecule. Close inspection of the cleavage pattern at T_5A_5 reveals that bands in the centre of this tract are cut better than those at the edges, even in the presence of low concentrations of distamycin. This becomes clearer at the higher ligand concentration.

Densitometer traces showing the results of similar experiments with Hoechst 33258 are shown in Figure 5c. The results are similar to those seen with distamycin. At the higher concentration (1 μM) two or three bands are evident at the centre of each $(A/T)_{10}$ tract, consistent with the suggestion that more than one ligand molecule is bound at each site. With the lower concentration (0.05 μM) a single region of attenuated hydroxyl radical cleavage is apparent in AATT, A_5T_5 and $(TA)_5$, as observed with distamycin. Once again the pattern at T_5A_5 is different, with cleavage products evident in the centre of this AT tract. It appears that even at this low concentration Hoechst 33258 binds more tightly to the edges than the centre of T_5A_5, thereby avoiding the TpA step.

$AT_{3–6}$

Although fragments AT_6 and AT_{10} allow us to compare the relative affinities of these ligands for different arrangements of AT residues, they cannot demonstrate the effect of site length on binding affinity. This is especially important since it appears that the longer AT tracts can accommodate more than one ligand molecule yet also contain TpA steps, which have previously been suggested to lower the binding strength. We therefore used fragment $AT_{3–6}$, which contains T_3, T_4, T_5 and T_6 tracts each separated by CGCG, to assess the influence of target site length on the binding affinity. The results of these experiments are presented in Figure 6. As expected these $A_n \cdot T_n$ tracts are resistant to DNase I cleavage, but a few weak bands are found within each site which can be used to demonstrate ligand binding and which have been analysed by densitometry. Although cleavage at T_3 and T_4 is strong enough to clearly identify ligand binding sites, bands are barely visible in the two longer sites. The results are best described using the C_{50} values presented in Table 2. Looking first at the results for distamycin it can be seen that the C_{50} value at T_3 is 2.4 ± 0.5 μM, higher than any value determined for the longer AT sites described above. Distamycin binds more tightly to T_4, producing a C_{50} value of 0.13 ± 0.03 μM. In contrast, lower concentrations are required to produce a footprint at T_5 and T_6. These two sites bind distamycin with similar affinities. With Hoechst

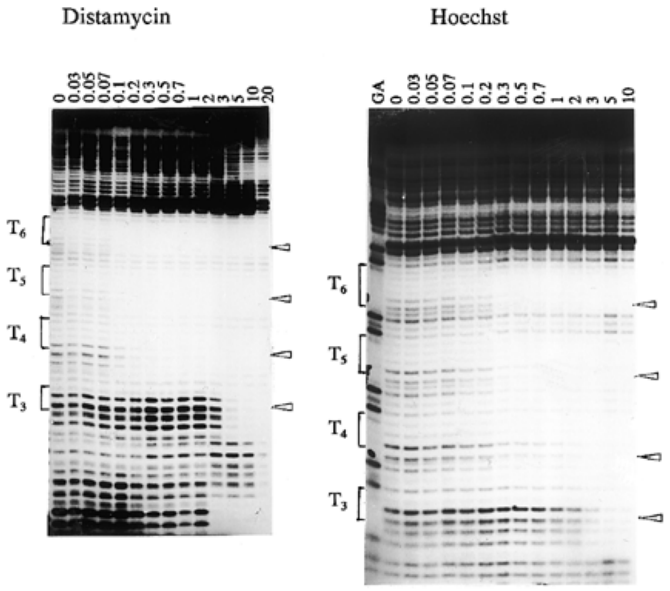

Figure 6. DNase I and hydroxyl radical cleavage patterns of fragment A_{3-6} in the presence of distamycin and Hoechst 33258. Ligand concentrations (μM) are indicated at the top of each lane. The position of each of the AT tracts is shown by the square brackets. The track labelled GA is a marker lane specific for purines. The arrows indicate the bands that were considered for quantitative analysis.

33258 T_3 is again the weakest site, as expected, with a C_{50} value of 1.2 ± 0.45 μM. T_4 is also a poor site, with a C_{50} of 0.098 ± 0.040 μM. In contrast, both T_5 and T_6 are strong binding sites, with C_{50} values of 0.053 ± 0.007 and 0.064 ± 0.007 μM respectively.

DISCUSSION

The results presented in this paper show that both Hoechst 33258 and distamycin discriminate between different arrangements of AT residues in both $(A/T)_6$ and $(A/T)_{10}$ tracts. Comparison of the various binding sites has been facilitated by using DNA fragments containing multiple ligand binding sites as footprinting substrates. Since the different AT binding sites within each fragment are located in very similar sequence environments and are each exposed to the same ligand concentration, the different footprinting profiles must reflect variations in the ligand binding constants. It should be noted that comparison of sites *within* each DNA fragment in this manner is much more reliable than comparison *between* fragments. In this Discussion we will consider the interaction of these ligands with $(A/T)_6$ and $(A/T)_{10}$ in turn.

$(A/T)_6$

DNase I footprinting with this fragment suggests that distamycin binds best to TAATTA, though it should be remembered that no binding data were obtained at A_3T_3 on account of its poor cleavage by the enzyme. Other studies comparing the binding of distamycin to fragments containing the inserts $CGCA_3T_3GCG$ and $CGCT_3A_3GCG$ (not shown) reveal that distamycin binds more tightly to the former site. TAATTA was included in fragment $(TA)_6$ since our previous work had suggested that flanking YR steps reduce the affinity for minor groove ligands by virtue of their effect on minor groove width. We therefore reasoned that TAATTA might be an inferior site to GAATTC; the present studies show that this is not the case. However, this may not be surprising since distamycin has a binding site size of five bases, so that the increase in affinity probably arises from the additional AT base pairs. It seems reasonable to assume that A_3T_3 will also be a good site since hydroxyl radical cleavage in this region is attenuated at the lowest ligand concentration. The improved binding on changing from $(TA)_3$ to TAATTA further emphasizes that AATT is a tighter binding site than ATAT and TATA, as previously demonstrated (27). The lack of difference between T_3A_3 and $(TA)_3$ is surprising since these sites contain one and three TpA steps respectively. It seems unlikely that this is due to distamycin binding across only half the site in either case (i.e. to GTTT or GTAT) as the data with A_{3-6} confirm that three contiguous AT base pairs constitute a poor distamycin binding site. It should also be noted that the hydroxyl radical footprints at T_3A_3 and $(AT)_3$ are in similar positions, suggesting that distamycin binds at the same position within each of these $(A/T)_6$ tracts. It therefore appears that central TpA steps have a greater effect on the binding affinity than those towards the edge of the binding site.

It should also be remembered that several studies have shown that distamycin can bind in a 2:1 mode at certain AT sequences, with two ligand molecules lying side by side in a widened minor groove. The present studies cannot distinguish between these binding modes, but merely show the overall affinity of the ligand for different AT sites. Indeed, it is possible that low and high concentrations of the ligand bind by different mechanisms and may be responsible for the total abolition of DNase I cleavage observed with high concentrations of distamycin but not Hoechst 33258. A full binding analysis, which is not warranted by the quality of data obtained from footprinting studies, would need to consider both binding modes. The departure from simple binding conditions might explain why some of the binding curves appear to be non-hyperbolic. The change in binding mode may also explain the higher than expected affinity at $(TA)_3$, since previous studies suggest that distamycin can bind to this site in the 2:1 mode (20), while either the 2:1 or 1:1 mode may be adopted at T_3A_3 and A_3T_3.

Hoechst 33258 has a smaller binding site size than distamycin (4 instead of 5 bp), it is therefore not surprising that TAATTA and GAATTC have the same affinity, since in both cases the ligand is binding to the central AATT. NMR studies have previously shown that Hoechst 33258 binds at a unique location in TAATTA, covering the central AATT (26). The lower affinities of T_3A_3 and $(TA)_3$ emphasize that the ligand avoids the TpA step, though once again three TpA steps in $(TA)_3$ are no weaker than one in T_3A_3. However, it is possible that in $(TA)_3$ the ligand is binding to the central tetranucleotide ATAT containing only one TpA step, since our previous studies have shown that the ligand binds more tightly to ATAT than TATA. Once again, it is not possible to determine whether A_3T_3 is any tighter than the other sites.

$(A/T)_{10}$

DNase I footprinting with this fragment reveals that distamycin binds to AATT more tightly than T_5A_5, even though the latter has the potential for binding two adjacent ligand molecules in each T_5 half. Experiments with fragments containing the inserts CA_5T_5G and CT_5A_5G (not shown) suggest that distamycin binds marginally more tightly to the latter. We can explain this result by referring to

the suggestion that the minor groove of A_n tracts narrows towards the 3′-end (29). A_5T_5 will therefore be narrowest at the centre, while, ignoring the effect of flanking sequences, T_5A_5 will be narrowest at the edges. It should therefore be easier to bind two contiguous distamycin molecules in each of the A_5 tracts in T_5A_5. This may in part explain why the binding of two ligand molecules is observed with T_5A_5 even at low concentrations, while at low concentrations A_5T_5 binds a single distamycin towards the centre.

Distamycin binds to the centre of $(TA)_5$ at least as well as to AATT, despite our previous observation that TATA and ATAT are poor distamycin binding sites. Binding to the edges of $(TA)_5$ is much weaker, more like that observed at isolated TATA and ATAT sites (27). Hydroxyl radical footprinting confirms that at low concentrations distamycin binds preferentially at the centre of the $(TA)_5$ tract. If all the TATA sites within the $(TA)_5$ tract were equivalent then we would expect distamycin to produce an even attenuation of hydroxyl radical cleavage throughout the insert. The centre of the $(TA)_5$ tract must therefore possess an unusual property which renders it a good distamycin binding site.

Hoechst 33258 also binds more tightly to AATT than T_5A_5, even though the latter could easily accommodate two Hoechst molecules, one in each A_5 tract. This is again consistent with our previous suggestion that AATT is an unusually good binding site for this ligand, tighter than AAAA. In addition, the hydroxyl radical data show clearly that at all concentrations Hoechst binds to the A_5 tracts rather than across the TpA step in the centre. Once again, binding to the centre of $(TA)_5$ is surprisingly good; the C_{50} value is a minimum at AT-3 and rises on either side of this. This again suggests that the centre (but not the edge) of an alternating AT tract possesses a structure which is favourable for minor groove binding. In this case an explanation in terms of 2:1 binding seems less likely since there is less evidence for Hoechst adopting this binding mode, though we cannot exclude this possibility (30). The binding to the edge of $(TA)_5$ more closely resembles that to isolated TATA and ATAT. Even though Hoechst 33258 binds better to the centre than to the edges of $(TA)_3$, this is still weaker than to AATT in the same fragment (Table 2), which is protected at lower ligand concentrations (Fig. 3). This further emphasizes that AATT is an unusually good binding site for Hoechst 33258 and contrasts with distamycin, for which the apparent affinity at the centre of $(AT)_3$ is similar to that at AATT.

Comparison with structural data

Although there have been many crystallographic and NMR studies on the binding of minor groove binding ligands to short oligonucleotides, most of these have used sequences containing the central sequence AATT (or AAATTT) (31). It is therefore not possible to directly compare the present results with known structural data. However, crystal structures have been reported for netropsin (10) and Hoechst 33258 (31) bound to CGCGAT-ATCGCG, which provide some clues about differences in the interaction of distamycin and Hoechst 33258 with alternating AT tracts. In the netropsin structure the helical twist alternates between ApT (33°) and TpA (39°), as expected for an alternating AT tract. This alternation is reversed by Hoechst 33258 so that ApT has a larger twist (39°) than TpA (31°). It appears that netropsin can bind to alternating AT tracts without distorting their structure, whereas Hoechst causes a change in DNA conformation, which may account for its weaker binding to regions of alternating AT. In contrast, several studies have shown that minor groove binding ligands have little effect on the structure of AATT. In addition, one report of netropsin bound to CGCGTTAACGCG (33) shows few differences between the structure of the drug-bound and free oligonucleotide. It is clear that further high resolution studies are required in order to understand how these ligands discriminate between different AT tracts.

ACKNOWLEDGEMENTS

This work was supported by grants from the Cancer Research Campaign and the Medical Research Council.

REFERENCES

1 Kopka,M.L. and Larsen,T.A. (1992) In Propst,C.L. and Perun,T.J. (eds), *Nucleic Acids Targeted Drug Design*. Marcel Dekker Inc., New York, NY, pp. 303–374.
2 Lown,J.W. (1993) In Neidle,S. and Waring,M.J. (eds), *Molecular Aspects of Anticancer Drug–DNA interactions*. Macmillan, London, UK, Vol. 1, pp. 322–355.
3 Van Dyke,M.W., Hertzberg,R.P. and Dervan,P.B. (1982) *Proc. Natl. Acad. Sci. USA*, **79**, 5470–5474.
4 Van Dyke,M.W. and Dervan,P.B. (1983) *Cold Spring Harbor Symp. Quant. Biol.*, **47**, 347–353.
5 Fox,K.R. and Waring,M.J. (1984) *Nucleic Acids Res.*, **12**, 9271–9285.
6 Portugal,J. and Waring,M.J. (1987) *FEBS Lett.*, **225**, 195–200.
7 Portugal,J. and Waring,M.J. (1987) *Eur. J. Biochem.*, **167**, 281–289.
8 Kopka,M.L., Yoon,D., Goodsell,D., Pjura,P. and Dickerson,R.E. (1985) *J. Mol. Biol.*, **183**, 553–563.
9 Kopka,M.L., Yoon,D., Goodsell,D., Pjura,P. and Dickerson,R.E. (1985) *Proc. Natl. Acad. Sci. USA*, **82**, 1376–1380.
10 Coll,M., Aymami,J., Van der Marel,G.A., van Boom,J.H., Rich,A. and Wang,A.H.-J. (1989) *Biochemistry*, **28**, 310–320.
11 Churchill,M.E.A., Hayes,J.J. and Tullius,T.D. (1990) *Biochemistry*, **29**, 6043–6050.
12 Zimmer,C., Marck,C., Schneider,C. and Guschlbauer,W. (1979) *Nucleic Acids Res.*, **6**, 2831–2837.
13 Ward,B. Rehfuss,R., Goodisman,J. and Dabrowiak,J.D. (1988) *Biochemistry*, **27**, 1198–1205.
14 Coll,M., Frederick,C.A., Wang,A.H.-J. and Rich,R. (1987) *Proc. Natl. Acad. Sci. USA*, **84**, 8385–8389.
15 Pelton,J.G. and Wemmer,D.E. (1989) *Proc. Natl. Acad. Sci. USA*, **86**, 5723–5727.
16 Pelton,J.G. and Wemmer,D.E. (1990) *J. Am. Chem. Soc.*, **112**, 1393–1399.
17 Pelton,J.G. and Wemmer,D.E. (1990) *J. Biomol. Struct. Dyn.*, **8**, 81–97.
18 Mkrsich,M. and Dervan,P.B. (1993) *J. Am. Chem. Soc.*, **115**, 2572–2576.
19 Fagan,P.A. and Wemmer,D.E. (1992) *J. Am. Chem. Soc.*, **114**, 1080–1081.
20 Geierstanger,B.H. and Wemmer,D.E. (1995) *Annu. Rev. Biophys. Biomol. Struct.*, **24**, 463–493.
21 Rentzeperis,D., Marky,L.A., Dwyer,T.J., Geierstanger,B.H., Pelton,J.G. and Wemmer,D.E. (1995) *Biochemistry*, **34**, 2937–2945.
22 Harshmann,K.D. and Dervan,P.B. (1985) *Nucleic Acids Res.*, **13**, 4825–4825.
23 Portugal,J. and Waring,M.J. (1988) *Biochim. Biophys. Acta*, **949**, 158–168.
24 Murray,V. and Martin,R.F. (1988) *J. Mol. Biol.*, **203**, 63–73.
25 Murray,V. and Martin,R.F. (1994) *Nucleic Acids Res.*, **22**, 506–513.
26 Embrey,K.J., Searle,M.S. and Craik,D.J. (1993) *Eur. J. Biochem.*, **211**, 437–447.
27 Abu-Daya,A., Brown,P.M. and Fox,K.R. (1995) *Nucleic Acids Res.*, **23**, 3385–3392.
28 Dabrowiak,J.C. and Goodisman,J. (1989) In Kallenbach,N.R. (ed.), *Chemistry and Physics of DNA–Ligand Interactions*. Adenine Press, New York, NY, pp. 143–174.
29 Burkhoff,A.M. and Tullius,T.D. (1987) *Cell*, **48**, 935–943.
30 Loontiens,F.G., Regenfuss,P., Zechel,A., Dumortier,L. and Clegg,R.M. (1990) *Biochemistry*, **29**, 9029–9039.
31 Tabernero,L., Bella,J. and Alemán,C. (1996) *Nucleic Acids Res.*, **24**, 3458–3466.
32 Carronda,M.A., Coll,M., Aymami,J., Wang,A.H.-J., van der Marel,C.A., van Boom,J.H. and Rich,A. (1989) *Biochemistry*, **28**, 7849–7859.
33 Balendiran,K., Rao,S.T., Sekharudu,Y., Zon,G. and Sundaralingam,M. (1995) *Acta Crystallogr.*, **51D**, 190–198.